

Title	Quantitative laser diffraction method for the assessment of protein subvisible particles
Author(s)	Totoki, Shinichiro; Yamamoto, Gaku; Tsumoto, Kouhei; Uchiyama, Susumu; Fukui, Kiichi
Citation	Journal of Pharmaceutical Sciences. 104(2) P.618-P.626
Issue Date	2015-01-01
Text Version	publisher
URL	<a href="http://hdl.handle.net/11094/79033">http://hdl.handle.net/11094/79033</a>
DOI	10.1002/jps.24288
rights	This article is licensed under a Creative Commons Attribution 4.0 International License.
Note	

*Osaka University Knowledge Archive : OUKA*

<https://ir.library.osaka-u.ac.jp/>

Osaka University

# Quantitative Laser Diffraction Method for the Assessment of Protein Subvisible Particles

SHINICHIRO TOTOKI,<sup>1</sup> GAKU YAMAMOTO,<sup>2</sup> KOUHEI TSUMOTO,<sup>3,4</sup> SUSUMU UCHIYAMA,<sup>2,5</sup> KIICHI FUKUI<sup>2</sup><sup>1</sup>Shimadzu Corporation, Kyoto 604-8511, Japan<sup>2</sup>Graduate School of Engineering, Osaka University, Suita, Osaka 565-0871, Japan<sup>3</sup>Institute of Medical Science, The University of Tokyo, Minato-ku, Tokyo 108-8639, Japan<sup>4</sup>Department of Chemistry & Biotechnology, The University of Tokyo, Minato-ku, Tokyo 108-8639, Japan<sup>5</sup>Okazaki Institute for Integrative Bioscience, Myodaiji, Okazaki, Aichi 444-8787

Received 31 August 2014; revised 27 October 2014; accepted 3 November 2014

Published online 1 December 2014 in Wiley Online Library (wileyonlinelibrary.com). DOI 10.1002/jps.24288

**ABSTRACT:** Laser diffraction (LD) has been recognized as a method for estimating particle size distribution. Here, a recently developed quantitative LD (qLD) system, which is an LD method with extensive deconvolution analysis, was employed for the quantitative assessment of protein particles sizes, especially aimed at the quantification of 0.2–10  $\mu\text{m}$  diameter subvisible particles (SVPs). The qLD accurately estimated concentration distributions for silica beads with diameters ranging from 0.2 to 10  $\mu\text{m}$  that have refractive indices similar to that of protein particles. The linearity of concentration for micrometer-diameter silica beads was confirmed in the presence of a fixed concentration of submicrometer diameter beads. Similarly, submicrometer-diameter silica beads could be quantified in the presence of micrometer-diameter beads. Subsequently, stir- and heat-stressed intravenous immunoglobulins were evaluated by using the qLD, in which the refractive index of protein particles that was determined experimentally was used in the deconvolution analysis. The results showed that the concentration distributions of protein particles in SVP size range differ for the two stresses. The number concentration of the protein particles estimated using the qLD agreed well with that obtained using flow microscopy. This work demonstrates that qLD can be used for quantitative estimation of protein aggregates in SVP size range. © 2014 The Authors. *Journal of Pharmaceutical Sciences* published by Wiley Periodicals, Inc. and the American Pharmacists Association *J Pharm Sci* 104:618–626, 2015

**Keywords:** laser diffraction method; proteins; protein aggregation; biopharmaceutical characterization; subvisible particles; imaging methods; particle size

## INTRODUCTION

Biopharmaceuticals such as antibody drugs have been successfully and widely used.<sup>1,2</sup> In particular, the range of clinical applicability of antibody drugs for treating autoimmune diseases and cancers has been expanded because of the high specificity and low adverse effect of these drugs. A fraction of antibodies is denatured during production, purification, and storage, leading to the formation of protein aggregates. Recently, risk of protein aggregates immunogenicity *in vivo* has been pointed out; thus, proper monitoring and suppression of the aggregates is expected. Assessment of protein aggregates has been discussed,<sup>3,4</sup> based on which the aggregates are divided into four categories according to the particle size: diameters below 0.2  $\mu\text{m}$  (200 nm), from 0.2 to 2  $\mu\text{m}$ , from 2 to 10  $\mu\text{m}$ , and from 10 to 25  $\mu\text{m}$ .<sup>5</sup> Quantitative assessment of protein particles with diameters below 200 nm, or more strictly below 100 nm, can be achieved by employing orthogonal meth-

ods including size-exclusion chromatography (SEC), analytical ultracentrifugation (AUC),<sup>6,7</sup> and field flow fractionation (FFF). Protein particles with diameters in the 10–25  $\mu\text{m}$  range can be assessed by employing light obscuration (LO) or microscopic observation. However, accurate quantification of protein particles with diameters in the subvisible particle (SVP) size range, especially in the 0.2–10  $\mu\text{m}$  range, remains a challenge, although flow microscopy technique is becoming a promising method for quantitative assessment of protein particle sizes in the 2–10  $\mu\text{m}$  diameter range.<sup>8–10</sup> FFF and Coulter counter might be effective for evaluating submicron protein particle diameters.<sup>11–14</sup> Recently, nanoparticle tracking analysis (NTA) and resonance mass measurement (RMM) were given significant attention for their potential use for assessing the protein particle sizes in the 0.2–2  $\mu\text{m}$  diameter range. In NTA, light scattered from individual particles in the object field is continuously tracked to estimate translational diffusion coefficients of the particles from which their hydrodynamic diameters are calculated using Stokes–Einstein equation, assuming Brownian motion and ideally spherical particles.<sup>10,15</sup> NTA allows measuring particle diameters ranging from about 0.2–1  $\mu\text{m}$ ; however, the technique is not suitable for assessing mixtures of particles with broad distribution of sizes, because estimating the signals from small particles becomes difficult because of intense light scattered from large particles. RMM allows measuring particle diameters ranging from about 0.2–8  $\mu\text{m}$  by using nanosensors, whereas particle diameters ranging from about 0.2–2  $\mu\text{m}$  can be measured using microsensors when densities of water and protein particles are 1.00 and

Correspondence to: Susumu Uchiyama (Telephone: +81-6879-4216; Fax: +81-6879-7442; E-mail: suchi@bio.eng.osaka-u.ac.jp)

This article contains supplementary material available from the authors upon request or via the Internet at <http://onlinelibrary.wiley.com/>.

*Journal of Pharmaceutical Sciences*, Vol. 104, 618–626 (2015)

© 2014 The Authors. *Journal of Pharmaceutical Sciences* published by Wiley Periodicals, Inc. and the American Pharmacists Association

This is an open access article under the terms of the Creative Commons Attribution-NonCommercial-NoDerivs License, which permits use and distribution in any medium, provided the original work is properly cited, the use is non-commercial and no modifications or adaptations are made.

1.37 g/mL, respectively. In RMM, the buoyant mass of a particle is quantified; thus, the RMM is advantageous for discriminating particles with partial-specific volumes larger than that of a solvent molecule from those with partial-specific volumes smaller than that of a solvent molecule.<sup>16,17</sup> In addition, none of the above methods can provide concentration distributions of protein particles in the whole 0.2–10  $\mu\text{m}$  diameter range. Laser diffraction (LD) method has been recognized as a method for estimating the relative size distribution of particles. In the present study, a recently developed quantitative LD system (qLD), which is an LD method that uses extensive deconvolution analysis, was employed for simultaneously assessing the concentration distributions of protein particles with diameters in the 0.2–10  $\mu\text{m}$  range.

## MATERIALS AND METHODS

### Materials

#### Silica Particles

Silica standard particles with diameters of 0.2  $\mu\text{m}$  (200 nm), 0.5  $\mu\text{m}$  (500 nm), and 1  $\mu\text{m}$  were purchased from micromod Partikeltechnologie GmbH (Rostock, Germany), whereas the particles with diameters of 3 and 5  $\mu\text{m}$  were purchased from Polysciences, Inc. (Warrington, Pennsylvania). Diameters of silica standard particles were confirmed by the manufacturer by using photon correlation spectroscopy for 0.2, 0.5, and 1  $\mu\text{m}$  diameter particles as  $0.2 \pm 0.02$ ,  $0.5 \pm 0.05$ , and  $1 \pm 0.1$   $\mu\text{m}$ . Values for 3 and 5  $\mu\text{m}$  diameter particles were measured by the manufacturer by using Coulter counter as  $3.20 \pm 0.37$  and  $5.06 \pm 0.44$   $\mu\text{m}$ . The weight concentrations of these particles were gravimetrically measured by the manufacturers. These standard particles are not NIST traceable. The number concentrations of these silica particles were estimated from the calculation that used the density of silica ( $2.0 \text{ g/cm}^3$ ), the weight concentrations of each silica particle solution, and the diameters, as provided by the manufacturers.

Particles were diluted with water before use. Silica particles in sucrose aqueous solution with sucrose concentrations of 30%, 35%, 40%, 45%, 50%, 55%, and 60% (w/w) were prepared. Sucrose was purchased from Wako Pure Chemical Industries, Ltd. (Osaka, Japan).

#### Intravenous Immunoglobulin

For an intravenous immunoglobulin (IVIG) sample, Glovenin-I for intravenous injection (250 units), a freeze-dried polyethylene glycol-treated human immunoglobulin G, was purchased from Nihon Pharmaceutical Company, Ltd. (Tokyo, Japan). Glovenin-I was reconstituted by using the supplied solvent followed by extensive dialysis against phosphate-buffered saline (PBS; pH 7.4) with Slide-A-Lyzer G2 Dialysis Cassettes, 10K MWCO, 3 mL (Thermo Scientific, Rockford, Illinois) to prepare a stock solution. The stock solution of protein was stored at 4°C and adjusted to 0.87, 4.35, and 8.7 mg/mL by dilution with PBS (pH 7.4) before use. The protein concentrations were determined using an extinction coefficient of 1.38 mL/mg cm. Particles of protein aggregates were generated by stir and heat stress. During the stir stress, 5 mL of the IVIG solution (0.87 mg/mL) was set in a batch cell (Fig. 1b) and stirred by a stirring blade ( $4.5 \times 29 \text{ mm}^2$ ) for 8 h at 190 strokes/min at room temperature. The prepared blade materials were glass, stain-

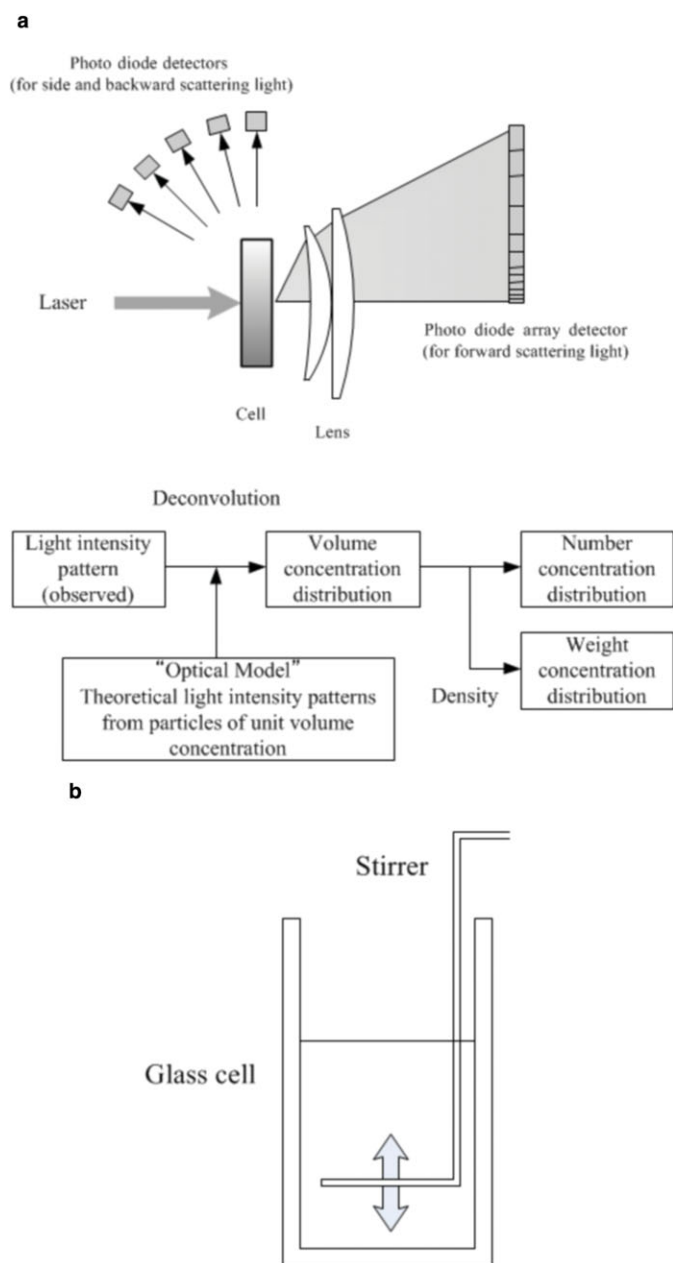


**Figure 1.** (a) Configuration and analysis flowchart for qLD instrument and (b) schematic drawing of a batch cell with stirring blade.

less steel (SUS316), and polyethelketone (PEEK). During the heat stress, 1 mL of the IVIG solution (0.87 mg/mL) in a 1.5-mL tube (Eppendorf Company, Ltd., Hamburg, Germany) was heated for 5, 7, 9, and 15 min at 70°C in a heater (CHT-101; SCINICS, Tokyo, Japan). The IVIG samples heated at 70°C for 15 min were used to prepare sucrose PBS (50 mM phosphate buffer, pH 7.4) solution with the sucrose concentrations, 40%, 45%, 50%, 55%, 60%, 65%, and 70% (w/w). Sucrose was purchased from Wako Pure Chemical Industries, Ltd.

### Methods

#### qLD Method

Particles in SVP size range were analyzed by employing the qLD method using Aggregates Sizer (Shimadzu Corporation,

Kyoto, Japan). Aggregates Sizer detects a scattered pattern, which is the intensity of light scattered from particles at different angles, ranging from  $0.04^\circ$  to  $160^\circ$ . The scattered pattern from a spherical particle with a particular diameter and a particular concentration in a solution can be theoretically expressed by using the quantitative optical model based on Mie scattering theory; this approach requires knowing the real and imaginary parts of refractive indices, for both the particles and the medium (the solvent). The total amount of scattered light from the particles is equal to the sum of the scattered light from individual particles, assuming that multiple scattering can be ignored in this range of concentrations. Thus, qLD provides the concentration distribution of particles in solution through deconvolution analysis of detected scattered pattern by using a program that employs the quantitative optical model. On the contrary, in conventional LD, the detected scattered pattern is analyzed with a program that uses the optical model in which the light intensity is normalized, resulting in relative size distribution. Detailed description of Mie scattering theory and deconvolution analysis is provided in Supporting Information. The estimated concentration distribution is volume-based distribution of particles. The volume concentration distribution can be converted into the weight concentration distribution by using the particles density. In addition, the volume concentration distribution can be converted into the number concentration distribution by using the equation for calculating the volume of a spherical particle using the particle diameter.

Conventional LD methods give normalized particle size distribution; however, with qLD, it is possible to obtain the particle size distribution with concentration information on particles with defined sizes. The wavelength of the laser light of the qLD, Aggregates Sizer, is 405 nm, allowing to effectively measure submicron diameter particles with higher sensitivity and resolution. Samples were analyzed either in a cell with a volume of 0.4 mL or in a cell with a volume of 5 mL, equipped with automatic stirring apparatus. A stirring blade made of stainless steel (SUS316), glass, or PEEK was used in the present study. The deconvolution analysis of acquired scattered patterns was performed by using the WingSALD bio software (version 3.1.5) provided by Shimadzu Corporation. The densities of  $2.00 \text{ g/cm}^3$  for silica beads and  $1.37 \text{ g/cm}^3$  for IVIG were used for converting the volume distribution into the weight distribution. The qLD measurements by the Aggregates Sizer can be performed by using both batch-type cell and flow-through-type cell.

### **Flow Microscopy**

A number of particles with diameters above  $1 \mu\text{m}$  were analyzed by using flow microscopy and employing DPA-4200 (Protein Simple, Santa Clara, California). The samples with their volumes ranging from 0.0778 to 0.1698 mL were analyzed to obtain the particle number concentrations.

### **Determination of Refractive Indices for Silica Beads and Protein Particles**

The scattered patterns from silica sucrose solution and IVIG sucrose solution were analyzed to determine the real parts of the corresponding refractive indices. For each concentration, sucrose refractive indices were measured using a refractometer (KPR-2000; Shimadzu Corporation) at the wavelength of 405 nm. The total scattered light intensity was calculated by summing the intensity detected by the photodiode array, rang-

ing from  $0.14^\circ$  to  $40^\circ$ , because the intensities in this range yield the information on the SVPs with diameters ranging from 0.1 to  $10 \mu\text{m}$ .

## **RESULTS AND DISCUSSION**

### **Number and Weight Concentration Distributions for Silica Beads Solution**

Estimation of size distribution by LD requires the refractive indices of particles for the wavelength used in the measurement. A previous study reported that the refractive indices of protein particles generated by stresses as 1.41.<sup>18</sup> On the contrary, the refractive indices of silica beads were estimated as 1.42,<sup>18</sup> which is close to those of the protein particles. It should be noted that the deconvolution analysis employing Mie theory requires the refractive indices of the particles and solvent at the wavelength used for the data acquisition and that, importantly, refractive index depends on the wavelength. In the present study, the Aggregates Sizer was equipped with laser light source at 405 nm. However, the above-mentioned reported values were obtained for wavelengths other than 405 nm, and were mostly refractive indices at 589 or 633 nm. In addition, the outcome from deconvolution analysis of scattered pattern in qLD is largely affected by the refractive indices of particle and solvent; thus, to infer the possibility of using the qLD for the quantitative assessment of protein particles, it is important to know whether the concentration distribution of silica beads can be properly quantified by using the qLD with appropriate refractive indices. So far, the refractive indices of neither silica beads nor protein particles have been reported at 405 nm; thus, we first measured the refractive indices at 405 nm of silica beads with different diameters. Figure 2a shows the total scattered light intensity detected by the Aggregates Sizer for silica sucrose solutions. The total intensity became minimal at the refractive index of 1.43, regardless of the silica beads diameter. This result is close to the value reported previously<sup>18</sup> and suggests that the real part of the refractive index of silica beads at 405 nm could be taken as 1.43. Then, the concentration distributions of silica beads were estimated by using the qLD, which was archived by the deconvolution analysis of scattered patterns acquired by the Aggregates Sizer, with the real and imaginary parts of the refractive index of silica beads estimated as 1.43 and 0, respectively, and the real and imaginary parts of the refractive index of the solvent estimated as 1.33 and 0, respectively. As shown in Figure 2b, for particle diameters below  $3 \mu\text{m}$ , as the diameter of the silica beads become larger, the peak position of the scattered light shifts from the larger numbered detector to the smaller numbered detector, implying that the scattering pattern changes from higher scattering weighted one to lower scattering weighted one. In the patterns obtained for 3 and  $5 \mu\text{m}$  diameter particles, diffraction from the particles was apparently confirmed at the higher numbered detector in addition to the scattered light at the lower numbered detector. Figure 2c (weight-based) and Supplementary Figure S1A (number-based) show the distribution estimates of silica beads, calculated from the deconvolution analysis of the scattered pattern, and the mean diameters of the particles are presented in Figure 2d and Supplementary Figure S1B. The mean diameter was consistent with the diameter provided by the manufacturer in a wide range of concentrations. Figure 2e and Supplementary Figure S1C show the weight and number

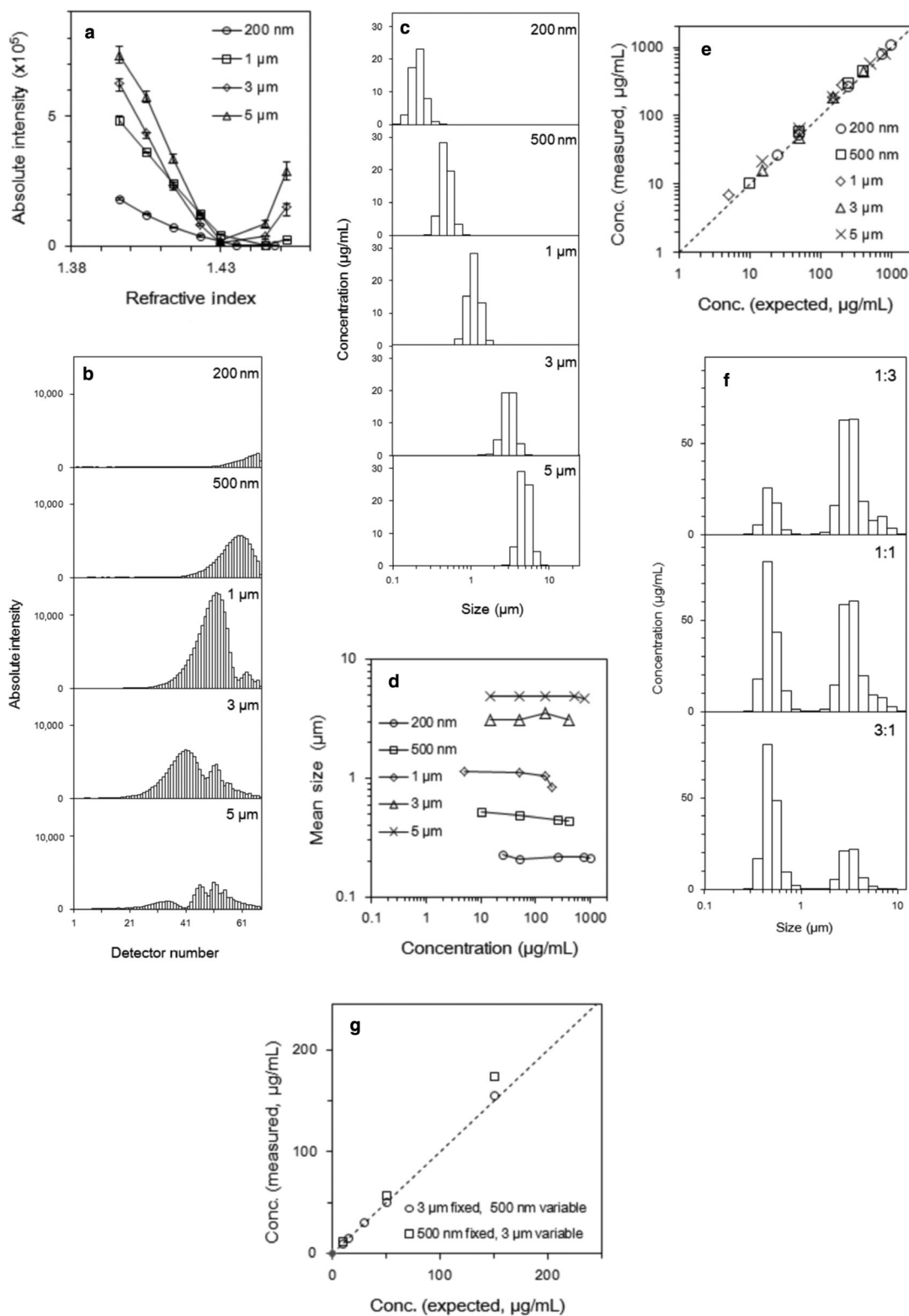


**Figure 2.** (a) Scattered light intensity of silica particles in sucrose solutions with different refractive indices. Error bars represent standard deviations from triplicate samples. Solutions were prepared in triplicates. (b) Representative scattered light intensity distribution and (c) particle size distribution of silica particles, obtained using the qLD. (d) Mean size of silica particles, for different particle concentrations, estimated using the qLD. (e) Expected weight concentrations versus weight concentrations obtained using the qLD method, for silica particles. (f) Representative particle size distributions for silica mixture particles estimated using the qLD. (g) Expected weight concentrations versus weight concentrations obtained using the qLD method, for silica particles mixtures. Silica particles of 0.5 and 3 μm diameters were mixed. Concentration of particles with a diameter was fixed at 150 μg/mL, whereas that of particles with another diameter was changed.



concentration estimates for each sample, respectively. The weight concentration estimates showed a linear relationship with the concentration calculated according to the value provided by the manufacturer. The measurement errors of weight concentration were below 30%, except for the 5- $\mu\text{m}$  diameter particles in low-concentration condition. On the contrary, the estimated number concentrations (Supplementary Fig. S1C) of particles with diameters above 1  $\mu\text{m}$  in high-concentration conditions significantly exceeded the expected values. This discrepancy from the expected values is possibly caused by multiple scattering that occurred in high-concentration conditions. These results indicate that the qLD allows correct quantifying of particle sizes and concentrations of subvisible range particles with diameters ranging from 0.2 to 10  $\mu\text{m}$ , within the appropriate range of concentrations. Subsequently, mixture solutions composed of different-size silica beads were evaluated by using the qLD. Figure 2f and Supplementary Figure S1D show the concentration distribution estimates for the mixture of submicrometer and micrometer diameter silica beads. Figure 2g and Supplementary Figure S1E show the weight and number concentration estimates, respectively, of 0.5  $\mu\text{m}$  diameter silica beads (circle) and of 3  $\mu\text{m}$  diameter silica beads (square) in the mixture. Results show that weight and number concentration estimates of 0.5  $\mu\text{m}$  diameter silica beads under a fixed concentration of coexisting 3  $\mu\text{m}$  diameter silica beads exhibit linear correlation with the corresponding concentration calculated according to the value provided by the manufacturer. The linear correlation was also confirmed for different weight and number concentration estimates of 3  $\mu\text{m}$  diameter silica beads in the presence of a fixed concentration of 0.5  $\mu\text{m}$  diameter silica beads.

#### Size Distribution with Concentration Information for IVIG Aggregates Solution

To determine the refractive indices of protein particles, the scattered pattern for sucrose solution containing heat- or shake-stressed IVIG was measured by using the Aggregates Sizer. As shown in Figure 3, scattered light intensities of both stressed samples attained minima at the refractive index of 1.46. Zolls et al.<sup>18</sup> had previously reported that the refractive index of protein particles is 1.41 for heat-stressed HSA aggregates and for stir-stressed IgG aggregates. Recall that the refractive index

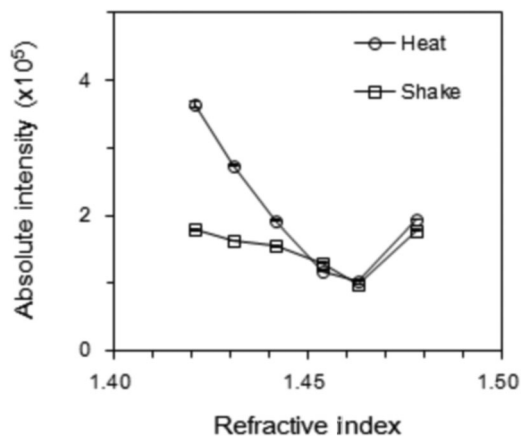


**Figure 3.** Scattered light intensity of the IVIG aggregates in sucrose solutions with different refractive indices. IVIG aggregates generated by heat or shake stress were tested.

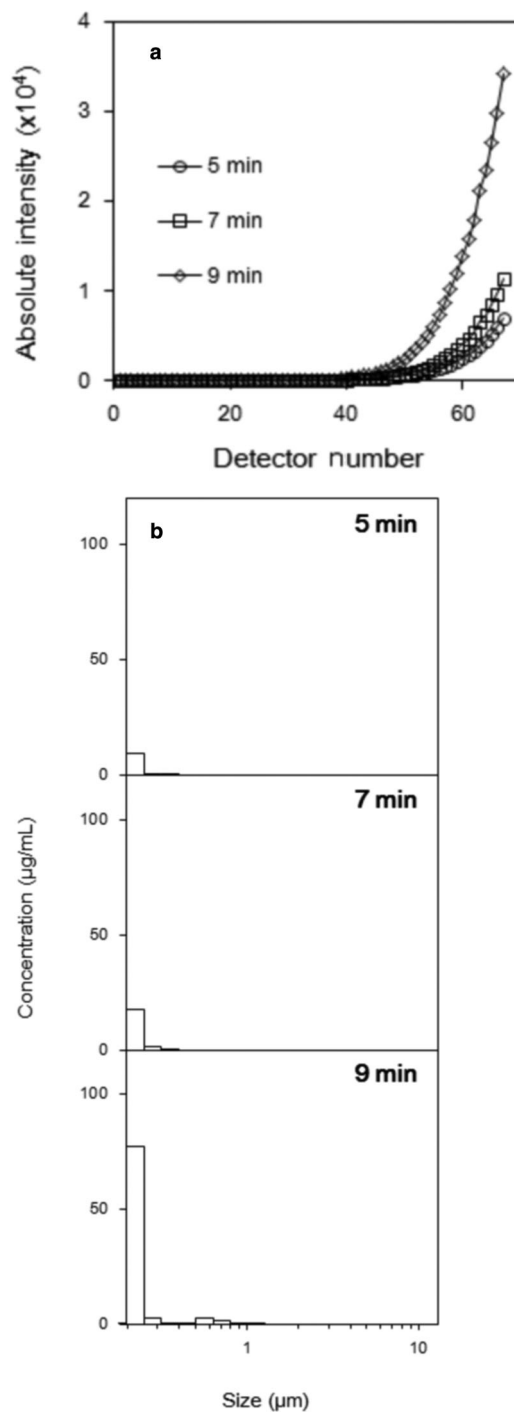


**Figure 4.** (a) Scattered light intensity distribution and (b) particle size distribution of the IVIG heat stressed at 70°C.

depends on the wavelength used for the measurement and that the Aggregates Sizer uses a laser beam at 405 nm, whereas the reported values are for 589 nm. Thus, in the present study, we used the experimentally determined refractive index of IVIG aggregates, 1.46 and 0.1 for the real and imaginary parts of the IVIG sample's refractive index, respectively. Figure 4a shows the scattered intensity, whereas the distribution estimates for heat-stressed IVIG sample are shown in Figure 4b (for weight concentration) and Supplementary Figure S2 (for number

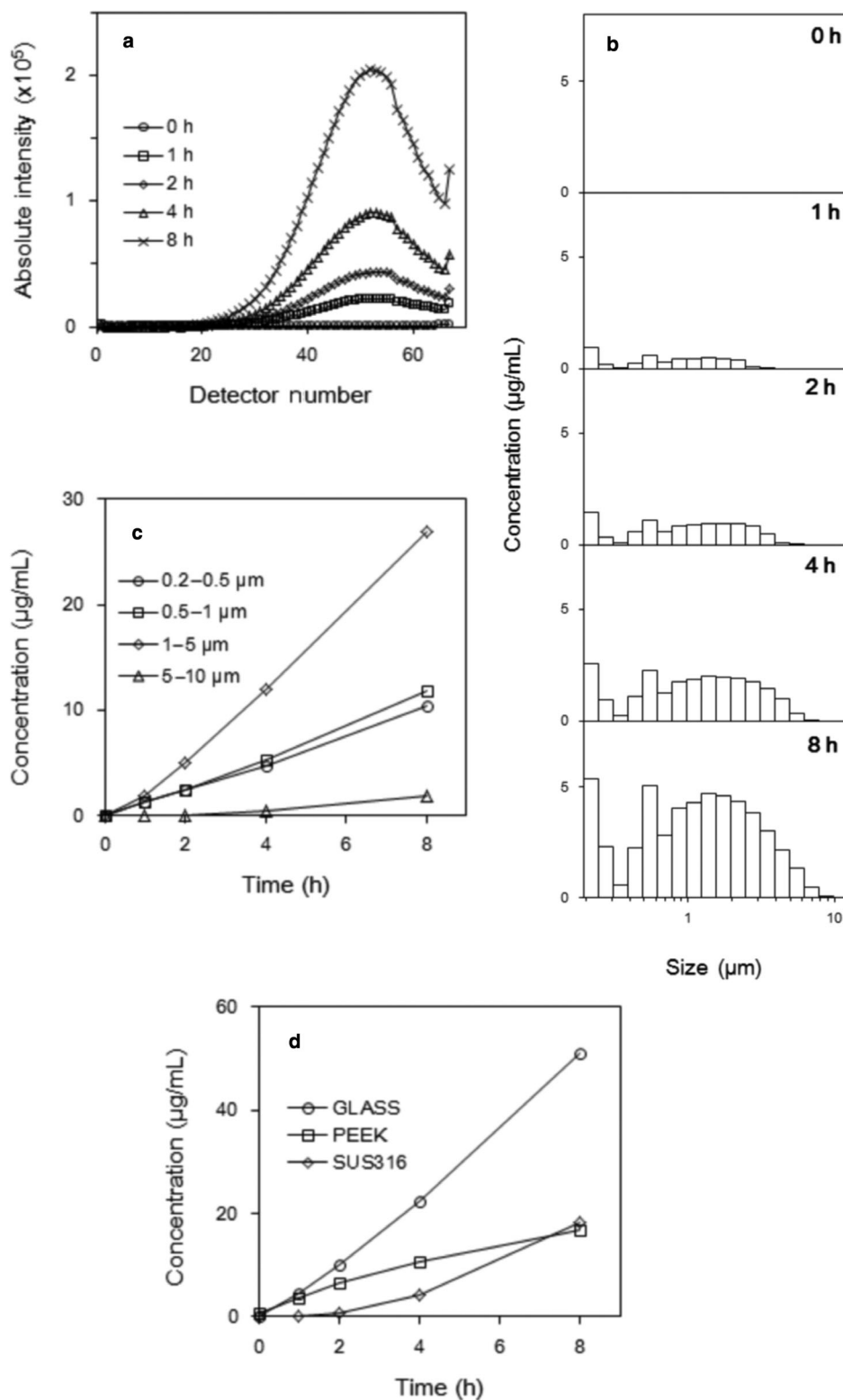


**Figure 5.** (a) Scattered light intensity distribution and (b) particle size distribution of the IVIG under stir stress in the batch cell with glass-made stirring blade. (c) Temporal dependence of concentration for the IVIG aggregates induced by stir stress in the batch cell with glass-made stirring blade. (d) Temporal dependence of concentration for the IVIG aggregates induced by stir stress in the batch cell with glass, PEEK, or SUS316-made stirring blade. Temporal results (c and d) were obtained from the deconvolution analysis of data taken by real-time qLD measurements.

concentration). Obviously, as illustrated in Figure 4a, increasing maximal scattered light intensity without any change in the apparent intensity profile shape was observed for longer heating duration, which corresponds to increasing particles concentration with increased heating duration. The scattered intensity patterns that were stronger at higher numbered detectors imply stronger presence of smaller diameter particles. In fact, the deconvolution analysis clearly yielded particles concentration increase at around the diameter of 0.2  $\mu\text{m}$ , whereas weaker presence of particles with diameters above 1  $\mu\text{m}$  was confirmed even when the heating duration increased (Fig. 4b; Supplementary Fig. S2). However, a stir-stressed IVIG sample exhibited different distributions, namely, scattered light intensity increased as the stirring time increased (Fig. 5a), whereas concentration distribution was apparently unchanged (Fig. 5b; Supplementary Fig. S3A). Regarding the particle formation by stir stress, the time-dependent weight concentration estimates obtained when the IVIG solution was stirred by using glass-made stirring blade are shown in Figure 5c and Supplementary Fig. S3B, and it is seen that the particle concentrations for different size range particles linearly increased with time. Notably, smaller size particles exhibited stronger increase in the corresponding number concentration (Supplementary Fig. S3B), whereas for the particles with diameters ranging from 1 to 5  $\mu\text{m}$ , the weight concentration exhibited the fastest growth. Size distributions of protein particles induced by heat, shake, and stir stress were previously investigated. Hawe et al.<sup>19</sup> reported a significant increase of particle number in submicrometer diameter range when the protein solution was heated. In fact, assuming that the density of protein aggregates is 1.37  $\text{g}/\text{cm}^3$ , the amount of heat-induced aggregates in micrometer diameter range calculated based on the number and size of aggregates counted by LO was less than 1% of total amount, whereas the amount of small aggregates, typically those with diameters below 100 nm, estimated from SEC, exceeded 10%. Filipe et al.<sup>20</sup> also showed that heat-induced aggregates have diameters of around 200 nm. On the contrary, stirring-induced aggregates had diameters in the micrometer range,<sup>21,22</sup> ranging from 1 to 5  $\mu\text{m}$  and from 2 to 10  $\mu\text{m}$ . In the present study, we demonstrated that the results were consistent with the results of the previous studies, in that the dominant increase of particle number in the submicrometer range diameter was obtained for heat-induced aggregates, whereas for the micrometer range diameter, the dominant increase was obtained for stirring-induced aggregates. The rate of the weight concentration increase obtained by using the glass-made stirring blade was faster than those achieved by using stainless steel or PEEK-made stirring blades (Fig. 5d; Supplementary Fig. S3C). It was pointed out that proteins tend to adsorb to form layers of films on the glass surface and the films are ruptured into solution,<sup>23</sup> constituting the major source of particles. The current result shows that the qLD can be utilized for the assessment of materials for stirring during protein production and purification. To confirm the concentration estimated by using the qLD method, the number concentration estimate by the qLD for IVIG heated at 70°C for 15 min was compared with that obtained by using flow microscopy. The result clearly demonstrated a good correspondence between the number concentration estimates obtained by using the qLD and flow microscopy, for particle diameters ranging from 1 to 5  $\mu\text{m}$  (Fig. 6). The potential error of flow microscopy originated from the volume used in this study is 20% according to the previous report.<sup>24</sup>

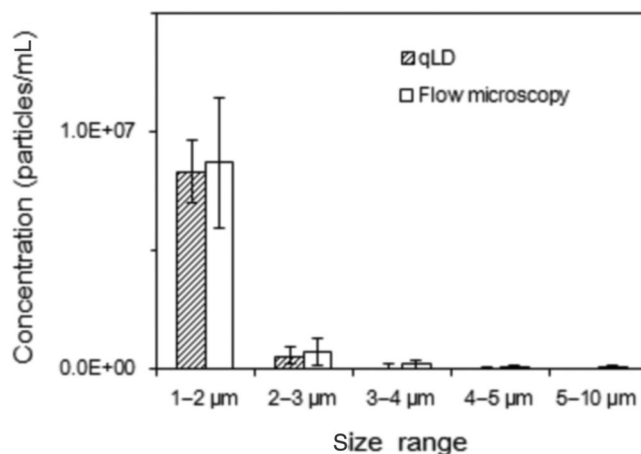


**Figure 6.** Number concentrations of the IVIG aggregates generated by heat stress at 70°C for 15 min, estimated using the qLD and flow microscopy. Error bars represent standard deviations from triplicate measurements.

Actual protein solution could contain particles other than proteins, such as silicone oil, glass, and metals. According to the report of Barnard et al.,<sup>25</sup> the maximal concentration of silicone oil particles derived from the container is  $2.3 \times 10^6$  particles/mL for particle diameters ranging from 0.4 to 2  $\mu\text{m}$ . Thus, we performed simulations to estimate the influence of silicone oil particles in the solution on the scattered light pattern obtained by using the qLD. Assuming that the refractive index and the concentration of silicone oil particles were 1.41 and  $2.3 \times 10^6$  particles/mL, respectively, we calculated the scattered light from silicone oil particles with diameters of 0.4, 1, and 2  $\mu\text{m}$ . As a result, the total scattered light intensities for the 0.4- $\mu\text{m}$  and the 1- $\mu\text{m}$  diameter particles were below the detection limit, whereas that for the 2- $\mu\text{m}$  diameter particles significantly affected the scattered light pattern.

#### Impact of Refractive Index on qLD Analysis

In the present study, we experimentally determined refractive indices of both silica beads and protein particles at 405 nm, and used them for the deconvolution analysis of the scattered pattern. We tested how a change in the refractive index affects the qLD results. As indicated in Supplementary Figure S4, when the real part of the refractive index of protein particles was changed from 1.46 to 1.44 or 1.48, corresponding to only 1.4% change of the value, the number concentration of particles in the 0.2–2- $\mu\text{m}$  diameter range changed by 23% for 1.44 and by 18% for 1.48, whereas the number concentration of particles in the 2–10- $\mu\text{m}$  diameter range changed by approximately 12.4% for 1.44 and by 2% for 1.48. These results indicate that the effect of refractive index on the number of particles is stronger in the 0.2–2- $\mu\text{m}$  diameter range compared with the 2–10- $\mu\text{m}$  diameter range. These results demonstrate the importance of direct measurement of refractive indices for particles and solvents (medium) comprising a solution in qLD analysis.

#### Comparison of qLD with Other Methods

The comparison of qLD with other methods used for SVP assessment is summarized in Table 1. It is obvious that qLD allows quantitative estimation of particle size distributions in a wide range of particle sizes.



**Table 1.** Comparison Table of qLD and Other Methods

Method	Instrument (Manufacturer)	Size Range	Quantification	Concentration Range (Particles/mL)	Monitoring Under Stress Condition
Flow microscopy	MFI5200 (ProteinSimple)	1–70 $\mu\text{m}$	Yes	Up to $9 \times 10^5$ (@ 2.5 $\mu\text{m}$ )	No
Light obscuration	System 9703+ (Beckman)	1.2–150 $\mu\text{m}$	Yes	Up to $1.8 \times 10^4$	No
Resonant mass measurement	Archimedes (Affinity Biosensors)	0.05–5 $\mu\text{m}$	Yes	$10^4$ – $10^9$	No
Nanoparticle tracing analysis	NS500 (NanoSight)	0.03–1 $\mu\text{m}$	Yes	$10^6$ – $10^9$	No
Dynamic light scattering	ZetasizerNano ZS (Malvern)	0.0003–10 $\mu\text{m}$	No	–	No
Laser diffraction	SALD-7500nano (Shimadzu)	0.007–800 $\mu\text{m}$	No	–	No
Quantitative laser diffraction	Aggregates Sizer (Shimadzu)	0.04–20 $\mu\text{m}$	Yes	$10^7$ – $10^9$ (@ 0.5 $\mu\text{m}$ ) $10^5$ – $10^7$ (@ 3 $\mu\text{m}$ )	Yes (stir stress)

## CONCLUSION

We have successfully developed a qLD method that employs extensive deconvolution analysis of scattered light pattern detected in a wide range of scattered angles. With the experimentally determined refractive indices of silica beads or protein particles, we were able to correctly estimate the number and size of silica beads by using the qLD even when particles of different diameters coexisted in the solution, and the protein particles generated by heat stress and stir stress could also be quantified by using the proposed qLD. Batch cell with continuous stirring blade provided the temporal dependence of protein particle formation, from which a clue regarding the kinetic understanding of the protein aggregates formation could be obtained. Most importantly, the developed qLD allows simultaneously analyzing the particles with diameters ranging from 0.2 to 10  $\mu\text{m}$ ; thus, the proposed method is expected to be highly useful for the quantitative evaluation of protein aggregates in subvisible size range.

## ACKNOWLEDGMENTS

We would like to thank Dr. Haruo Shimaoka (Shimadzu corp.) for insightful comments during the research. This work was supported by Grant-in-Aid for Scientific Research on Innovative Areas (25440071) from MEXT and Manufacturing Technology Research of Biologics from METI to S. U.

## REFERENCES

- Nelson AL, Dhimolea E, Reichert JM. 2010. Development trends for human monoclonal antibody therapeutics. *Nat Rev Drug Discov* 9:767–774.
- Uchiyama S. 2014. Liquid formulation for antibody drugs. *BBA-Proteins and Proteomics* 1844:2041–2052.
- Singh SK, Afonina N, Awwad M, Bechtold-Peters K, Blue JT, Chou D, Cromwell M, Krause HJ, Mahler HC, Meyer BK, Narhi L, Nesta DP, Spitznagel T. 2010. An industry perspective on the monitoring of subvisible particles as a quality attribute for protein therapeutics. *J Pharm Sci* 99(8):3302–3321.
- Carpenter JF, Randolph T, Jiskoot W, Crommelin DJA, Middaugh CR, Winter G, Fan Y-X, Krishna S, Verthelyi D, Kozlowski S, Clouse KA, Swann PG, Rosenberg A, Cherney B. 2009. Overlooking subvisible particles in therapeutic protein products: Gaps that may compromise product quality. *J Pharm Sci* 98(4):1201–1205.
- FDA draft guidance. 2013. Immunogenicity assessment for therapeutic protein products.
- Carpenter JF, Randolph TW, Jiskoot W, Crommelin DJ, Middaugh CR, Winter G. 2010. Potential inaccurate quantitation and sizing of protein aggregates by size exclusion chromatography: Essential need to use orthogonal methods to assure the quality of therapeutic protein products. *J Pharm Sci* 99(5):2200–2208.
- Krayukhina E, Uchiyama S, Nojima K, Okada Y, Hamaguchi I, Fukui K. 2013. Aggregation analysis of pharmaceutical human immunoglobulin preparations using size-exclusion chromatography and analytical ultracentrifugation sedimentation velocity. *J Biosci Bioeng* 115(1):104–110.
- Sharma DK, King D, Oma P, Merchant C. 2010. Micro-flow imaging: Flow microscopy applied to sub-visible particulate analysis in protein formulations. *AAPS J* 12(3):455–464.
- Cordes AA, Carpenter JF, Randolph TW. 2012. Accelerated stability studies of abatacept formulations: Comparison of freeze–thawing- and agitation-induced stresses. *J Pharm Sci* 101:2307–2315.
- Joubert MK, Luo Q, Nashed-Samuel Y, Wypych J, Narhi LO. 2011. Classification and characterization of therapeutic antibody aggregates. *J Biol Chem* 286:25118–25133.
- Liu J, Andya JD, Shire SJ. 2006. A critical review of analytical ultracentrifugation and field flow fractionation methods for measuring protein aggregation. *AAPS J* 8(3):E580–E589.
- Gabrielson JP, Brader ML, Pekar AH, Mathis KB, Winter G, Carpenter JF, Randolph TW. 2007. Quantitation of aggregate levels in a recombinant humanized monoclonal antibody formulation by size-exclusion chromatography, asymmetrical flow field flow fractionation, and sedimentation velocity. *J Pharm Sci* 96(2):268–279.
- Rhyner MN. 2011. The coulter principle for analysis of subvisible particles in protein formulations. *AAPS J* 13(1):54–58.
- Demeule B, Messick S, Shire SJ, Liu J. 2010. Characterization of particles in protein solutions: Reaching the limits of current technologies. *AAPS J* 12(4):708–715.
- Filipe V, Poole R, Oladunjoye O, Braeckmans K, Jiskoot W. 2012. Detection and characterization of subvisible aggregates of monoclonal IgG in serum. *Pharm Res* 29:2202–2212.
- Patel AR, Lau D, Liu J. 2012. Quantification and characterization of micrometer and submicrometer subvisible particles in protein therapeutics by use of a suspended microchannel resonator. *Anal Chem* 84(15):6833–6840.
- Weinbuch D, Zolls S, Wiggernhorn M, Friess W, Winter G, Jiskoot W, Hawe A. 2013. Micro-flow imaging and resonant mass measurement (Archimedes)—Complementary methods to quantitatively

differentiate protein particles and silicone oil droplets. *J Pharm Sci* 102:2152–2165.

18. Zolls S, Gregoritza M, Tanatipolphan R, Wiggenhorn M, Winter G, Friess W, Hawe A. 2013. How subvisible particles become invisible—Relevance of the refractive index for protein particle analysis. *J Pharm Sci* 102:1434–1446.

19. Hawe A, Kasperb JC, Friess W, Jiskoot W. 2009. Structural properties of monoclonal antibody aggregates induced by freeze–thawing and thermal stress. *Eur J Pharm Sci* 38:79–87.

20. Filipe V, Jiskoot W, Basmeh AH, Halim A, Schellekens H, Brinks V. 2012. Immunogenicity of different stressed IgG monoclonal antibody formulations in immunotolerant transgenic mice. *mAbs* 4(6):740–752.

21. Kiese S, Pappenberg A, Friess W, Mahler HC. 2008. Shaken, not stirred: Mechanical stress testing of an IgG1 antibody. *J Pharm Sci* 97(10):4347–4365.

22. Ishikawa T, Kobayashi N, Osawa C, Sawa E, Wakamatsu K. 2010. Prevention of stirring-induced microparticle formation in monoclonal antibody solutions. *Biol Pharm Bull* 33(6):1043–1046.

23. Rudiuk S, Cohen-Tannoudji L, Huilleb S, Tribet C. 2012. Importance of the dynamics of adsorption and of a transient interfacial stress on the formation of aggregates of IgG antibodies. *Soft Matter* 8:2651–2661.

24. Zolls S, Weinbuch D, Wiggenhorn M, Winter G, Friess W, Jiskoot W, Hawe A. 2013. Flow imaging microscopy for protein particles analysis—A comparative evaluation of four different analytical instruments. *AAPS J* 15(4):1200–1211.

25. Barnard JG, Babcock K, Carpenter JF. 2012. Characterization and quantitation of aggregates and particles in interferon- $\beta$  products: Potential links between product quality attributes and immunogenicity. *J Pharm Sci* 102(3):915–928.